South East Asian J. of Mathematics and Mathematical Sciences
Vol. 19, No. 1 (2023), pp. 301-322

DOI: 10.56827/SEAJMMS.2023.1901.25 **ISSN (Online): 2582-0850**

ISSN (Print): 0972-7752

MATHEMATICAL ANALYSIS OF SVEIQR MODEL FOR COVID-19

Laxman Bahadur Kunwar and Vijai Shanker Verma*

Department of Mathematics,
Thakur Ram Multiple Campus, Tribhuvan University, Birgunj, NEPAL

E-mail : laxman.kunwar@trmc.tu.edu.np

*Department of Mathematics and Statistics
Deen Dayal Upadhyaya Gorakhpur University,
Gorakhpur - 273009, Uttar Pradesh, INDIA

E-mail : drvsverma01@gmail.com

(**Received:** *Feb. 21, 2023* **Accepted:** *Apr. 13, 2023* **Published:** *Apr. 30, 2023)*

Abstract: In this paper, we have proposed an SVEIQR compartmental model modifying the classical SEIR model with inclusion of vaccinated and quarantined classes to explain the COVID-19 outbreak mathematically. We have calibrated our model with the daily COVID-19 data reported by the WHO coronavirus dashboard. To observe the disease dynamics of COVID-19, a detailed stability analysis of the proposed SVEIQR model is carried out. Our results show that the disease free equilibrium (DFE) is stable if the basic reproduction number is less than unity and unstable otherwise. Moreover, endemic equilibrium (EE) is found to be stable when certain restrictions hold. The expression for effective reproduction number has been derived analytically and its value is calculated based on the reported cases. Sensitivity analysis of effective reproduction number is performed employing PRCCs and Latin hypercube scheme. We have compared short-term and long-term transmission dynamics of COVID-19 for India with different levels of vaccination and without control strategies. The impact of different degrees of control interventions is ascertained with the numerical simulation of the model.

Keywords and Phrases: COVID-19, Equilibrium point, Stability, Sensitivity analysis, Effective reproduction number, Numerical simulation.

2020 Mathematics Subject Classification: 34D20, 34D23, 34D08.

1. Introduction

The COVID-19 outbreak first surfaced in Wuhan, China, in the month of December 2019. The World Health Organization marked the illness as global pandemic on March 11, 2020. The WHO daily situational assessment states that since the very start of the virus outbreak, it was spreading rapidly and posing a serious threat to lives of people [31]. It has been noted that direct human contact is the primary method of COVID-19 transmission [2, 14, 33]. Daily statistics throughout the world has demonstrated that COVID-19 spreads almost exponentially in the early stages of the pandemic [16].

In India and around the world, the COVID-19 pandemic has caused significant damage. Its population dynamics are similar to the typical infection waves seen in previous respiratory pathogen pandemics, such as the influenza in 1918 and in 2009 [10, 26]. The first SARS-CoV-2 infection wave in India began in late January 2020 and lasted for nearly nine months. Over the course of this time, India has recorded a total of 11 million cases and 0.157 million deaths, with the peak occurring in mid-September 2020 [31]. This was actually moderate in comparison with the second wave, that started in mid-February 2021 and spread more explosively over the whole country. The advent of more contagious SARS-CoV-2 strains, namely B.1.1.7 (Alpha variant) and B.1.617.2 (Delta variant), of which the latter is the main factor generating this second wave [27]. This outbreak began shortly after the vaccination implementation, that began on January 16, 2021, and was further exacerbated by the opening of gathering places, widely dispersed events following massive gatherings after the first wave, and the lack of concern for personal protective measures (correct and a habit of use of face masks) [18].

There is currently growing discussion over the possibility of a subsequent wave of SARS-CoV-2 infection [27]. In other parts of the country, successive waves have emerged and may be influenced by a variety of causes. For instance, the third SARS-CoV-2 wave in the UK occurred in the winter of 2020, coinciding with the region's yearly influenza season in the northern hemisphere as well as occurring after the removal of lockdown restrictions [7, 12]. Furthermore, the persistent threat of viral evolution poses a potential recurrence in the future [28].

In anticipation to this pandemic, mathematical modeling has served a crucial role by providing estimates of the basic reproduction number across regions, analysis based on treatments incorporated in the models, quantifying illness severity, and more. The compartmental model developed by Kermack and McKendrick, which is subsequently expanded to other epidemiological models for COVID-19, serves as the basis for the vast majority of the works. By explaining many mathe-

matical models [15], Anirudh (2020) explored briefly the prediction of COVID-19, its growth, spread, and reduction. He also described the various problems and the results [1]. Saeed et al. (2021) have provided thorough information on a number of interventions for COVID-19 [21]. By presenting an SVIQR epidemic model for COVID-19, Verma et al. (2022) have explored the consequences of vaccination and other preventative interventions on the dynamics of coronavirus disease [30]. Bhadauria et al. (2022) investigated a straightforward model taking into account the capability of viruses to survive in their immediate environment [5].

In this study, we create an epidemiological model that incorporates natural births, deaths, vaccinations rate and infectious reduction of vaccinated individuals. The population is divided into six groups, which include susceptible, vaccinated, exposed, infected, quarantined and recovered. Home isolation and hospitalized populations are included in the quarantine class of infectious compartment. The main purpose of this study is to ascertain how reduced disease transmission rates can be achieved by increasing detection rates of asymptomatic and symptomatic unidentified persons. Here, we shall observe how the vaccination rate of susceptible individuals and other non-pharmaceutical interventions help to reduce disease transmission and, eventually, the basic reproduction ratio.

The main goal of this work is to apply a deterministic compartmental model to the patterns of the COVID-19 disease with the objective to analyze it, as well as to identify some preventative methods for controlling it from spreading.

2. Model Formulation

For the mathematical formulation of the model, we have divided the total population according to their disease status into six mutually exclusive epidemiological state compartments: susceptible $S(t)$, vaccinated $V(t)$, exposed $E(t)$, infected $I(t)$, quarantined $Q(t)$ and recovered $R(t)$ classes. The infected people who exhibit severe symptoms are hospitalized and part of the confined group. People who have successfully recovered from the COVID-19 disease and received a testing result of zero are considered to be in the recovered class. The population $N(t)$ at any time t is given by $N(t) = S(t) + V(t) + E(t) + I(t) + Q(t) + R(t)$. It has been seen that by close contact with an infected person who belongs to class $I(t)$ or in the $Q(t)$, a susceptible person may get infected. In theory, people who are quarantined or isolated are unable from passing on the virus to others who are susceptible persons, but in practice, we see that many members of the staff at quarantine and isolation facilities, including doctors, nurses, and other medical professionals, as well as their families, have caught the illness from such people.

The flow diagram of proposed SVEIQR model for COVID-19 is illustrated in Figure (1). The following set of differential equations captures the dynamics of

COVID-19 in the proposed SVEIQR model :

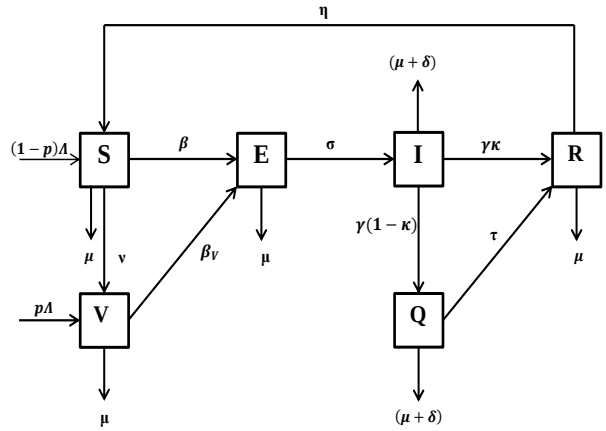

Figure 1: Compartmental diagram of SVEIQR model for COVID-19

$$\left.\begin{aligned}
\frac{dS(t)}{dt} &= (1-p)\Lambda + \eta R - (\beta+\mu+\nu)S,\\
\frac{dV(t)}{dt} &= p\Lambda + \nu S - (\beta_\nu+\mu)V,\\
\frac{dE(t)}{dt} &= \beta S + \beta_\nu V - (\sigma+\mu)E,\\
\frac{dI(t)}{dt} &= \sigma E - (\gamma+\mu+\delta)I,\\
\frac{dQ(t)}{dt} &= \gamma(1-\kappa)I - (\tau+\mu+\delta)Q,\\
\frac{dR(t)}{dt} &= \gamma\kappa I + \tau Q - (\eta+\mu)R
\end{aligned}\right\} \tag{1}$$

with $S(0) > 0, V(0) \geq 0, E(0) \geq 0, I(0) \geq 0, Q(0) \geq 0, R(0) \geq 0$.
In the above model, we assume $\beta = b\left(\frac{\omega_I I + \omega_Q Q}{N}\right)$ and $\beta_\nu = b(1-\varepsilon)\left(\frac{\omega_I I + \omega_Q Q}{N}\right)$, where b is the effective contact rate, ω_I and ω_Q represent the transmission probability of virus after contact with the individual in status I and Q respectively. The notation ε represents infectious reduction of vaccinated individuals. For the sake of simplicity, we shall also use the following notation :
$g_1 = \mu + \nu; g_2 = \mu; g_3 = \sigma + \mu; g_4 = \gamma + \mu + \delta; g_5 = \tau + \mu + \delta; g_6 = \eta + \mu$.

Table 1: Description of the parameters used in the system.

Parameter	Description
Λ	Recruitment rate of individuals into the population
p	Proportion of the recruitment individual who is vaccinated
ν	Vaccinated rate
β	The transmission rate from susceptible to exposed class
β_ν	The transmission rate from vaccinated to exposed class
μ	Natural death rate
δ	Disease-induced death rate
σ	Exists rate from the exposed class
κ	Proportion of the infectious who recovered naturally
τ	Recovered rate of quarantined individuals
η	Rate at which individual lose immunity
γ	Rate at which individual exists from the infectious class

Now, the system (1) can be re-written as follows :

$$\left.\begin{aligned}
\frac{dS(t)}{dt} &= (1-p)\Lambda + \eta R - (\beta + g_1) S, \\
\frac{dV(t)}{dt} &= p\Lambda + \nu S - (\beta_\nu + g_2) V, \\
\frac{dE(t)}{dt} &= \beta S + \beta_\nu V - g_3 E, \\
\frac{dI(t)}{dt} &= \sigma E - g_4 I, \\
\frac{dQ(t)}{dt} &= \gamma (1-\kappa) I - g_5 Q, \\
\frac{dR(t)}{dt} &= \gamma\kappa I + \tau Q - g_6 R
\end{aligned}\right\} \tag{2}$$

3. Model Analysis

3.1. Positivity of Solution

The COVID-19 outbreak model provided by system (1) must demonstrate that all state variables always remain positive for all $t \geq 0$ in order to be epidemiologically realistic. Thus, we have the following theorem:

Theorem 1. *Let* $F(t) = (S(t), V(t), E(t), I(t), Q(t), R(t))$ *and* $\mathbb{R}^6_+ = \{F(0) \in \mathbb{R}^6 : F(0) \geq 0\}$. *Then, the solution set* $F(t)$ *of the proposed SVEIQR model for*

COVID-19 model will be non-negative for all $t \geq 0$ *in* $\mathbb{R}^6_+$.

Proof. From the first equation of the system of equations (2), it is noted that

$$\frac{dS(t)}{dt} \geq -(\beta + g_1) S$$

which on integration provides $S(t) \geq S(0)e^{-(\beta+g_1)t}$.
Hence, we conclude that $S(t) \geq 0$ for all $t \geq 0$.
Continuing in the same manner, it can be proved that
$V(t) \geq 0, E(t) \geq 0, I(t) \geq 0, Q(t) \geq 0$ and $R(t) \geq 0$, for all $t \geq 0$.
Thus, the solution set falls into the hyperplane $F(t) = \{(S, V, E, I, Q, R) \in \mathbb{R}^6_+\}$.
Hence, the proposed SVEIQR model for COVID-19 is epidemiologically realistic.

3.2. Invariant Region

Here, we shall demonstrate that the proposed SVEIQR model is correctly laid out biologically and mathematically in the invariant set $F(t)$ and establish that the closed region $F(t)$ is a positively invariant.

Theorem 2. *The solution set of the system* (1) *with the initial conditions is stated in the* $F(t)$ *given by*

$$F(t) = \left\{ (S(t), V(t), E(t), I(t), Q(t), R(t)) \in \mathbb{R}^6_+ : 0 < N(t) \leq \frac{\Lambda}{\mu} \right\}$$

Proof. Taking the sum of the populations of all the six compartments, we get

$$N(t) = S(t) + V(t) + E(t) + I(t) + Q(t) + R(t). \tag{3}$$

Differentiating and using system of equations (2), we get

$$\frac{dN}{dt} = \Lambda - \mu N - \delta(I - \delta) Q$$

from which, we conclude that

$$\frac{dN}{dt} \leq \Lambda - \mu N. \tag{4}$$

By applying the theorem on the differential inequalities [6], the solution of (4) is obtained as

$$N(t) \leq \frac{\Lambda}{\mu} - \left(\frac{\Lambda}{\mu} - N_0 \right) e^{-\mu t} \tag{5}$$

where $N_0 = N(0)$, the initial population. Now, as $t \to \infty$, then from (5), we find that $N(t) \to \dfrac{\Lambda}{\mu}$ from which, it is concluded that $0 \leq N \leq \dfrac{\Lambda}{\mu}$. Thus, all the feasible solutions of model (1) converge in the region $F(t)$. Hence, we have

$$F(t) = \left\{ (S(t), V(t), E(t), I(t), Q(t), R(t)) \in \mathbb{R}^6_+ : 0 < N(t) < \frac{\Lambda}{\mu} \right\}.$$

3.3. Existence of Disease-Free Equilibrium (DFE)

For the existence of the disease-free equilibrium (DFE), we have

$$\frac{dS}{dt} = 0;\ \frac{dV}{dt} = 0;\ \frac{dE}{dt} = 0;\ \frac{dI}{dt} = 0;\ \frac{dQ}{dt} = 0;\ \frac{dR}{dt} = 0.$$

Using the system of equations (2), we get the following equations :

$$(1-p)\Lambda + \eta R - (\beta + g_1) S = 0 \tag{6}$$

$$p\Lambda + \nu S - (\beta_\nu + g_2) V = 0 \tag{7}$$

$$\beta S + \beta_\nu V - g_3 E = 0 \tag{8}$$

$$\sigma E - g_4 I = 0 \tag{9}$$

$$\gamma(1-\kappa) I - g_5 Q = 0 \tag{10}$$

$$\gamma\kappa I + \tau Q - g_6 R = 0 \tag{11}$$

For DFE, we put $I = 0$, so that from (9), (10) and (11), we get
$E = 0, Q = 0$, and $R = 0$.

Now, by taking $\beta = 0,\ \beta_\nu = 0$ and $R = 0$ in (6), we get $S = \dfrac{(1-p)\Lambda}{g_1}$.

Again, by using the value of S in equation (7), we get $V = \frac{\Lambda\{pg_1 + (1-p)\nu\}}{g_1 g_2}$.

Hence, the DFE is obtained as $E_1(S^0, V^0, E^0, I^0, Q^0, R^0)$, where

$$S^0 = \frac{(1-p)\Lambda}{g_1},\ V^0 = \frac{\Lambda\{pg_1 + (1-p)\nu\}}{g_1 g_2},\ E^0 = 0, I^0 = 0,\ Q^0 = 0,\ R^0 = 0$$

3.4. Basic Reproduction Number

The next generation matrix approach, put out by Diekmann *et. al.*, and Van den Driessche and Watmough, is a generalized method for calculating the basic reproduction number [9, 29]. Here, we break down the right-hand side of the system (2) that corresponds to the infected classes $E,\ I$, and Q as $\mathcal{F} - \mathcal{W}$, where

$$\mathcal{F} = \begin{bmatrix} \beta S + \beta_\nu V \\ 0 \\ 0 \end{bmatrix} = \begin{bmatrix} b\left(\dfrac{\omega_I I + \omega_Q Q}{N}\right) S + b(1-\varepsilon)\left(\dfrac{\omega_I I + \omega_Q Q}{N}\right) V \\ 0 \\ 0 \end{bmatrix}$$

and

$$\mathcal{W} = \begin{bmatrix} g_3 E \\ -\sigma E + g_4 I \\ -\gamma(1-\kappa) I + g_5 Q \end{bmatrix},$$

The non-negative matrix $\mathbf{F}$ and the non-singular matrix $\mathbf{W}$, for $x_j = E, I, Q$, representing the new infectious terms and remaining transfer terms are given by

$$\mathbf{F} = \left.\frac{\partial \mathcal{F}}{\partial x_j}\right|_{(E_1)} = \begin{bmatrix} 0 & b\frac{\omega_I}{N_0} S^0 + b(1-\varepsilon)\frac{\omega_I}{N_0} V^0 & b\frac{\omega_Q}{N_0} S^0 + b(1-\varepsilon)\frac{\omega_Q}{N_0} V^0 \\ 0 & 0 & 0 \\ 0 & 0 & 0 \end{bmatrix}$$

$$= \begin{bmatrix} 0 & b\frac{\omega_I}{N_0}\left(S^0 + (1-\varepsilon) V^0\right) & b\frac{\omega_Q}{N_0}\left(S^0 + b(1-\varepsilon) V^0\right) \\ 0 & 0 & 0 \\ 0 & 0 & 0 \end{bmatrix}$$

$$\mathbf{W} = \left.\frac{\partial \mathcal{W}}{\partial x_j}\right|_{(E_1)} = \begin{bmatrix} g_3 & 0 & 0 \\ -\sigma & g_4 & 0 \\ 0 & -\gamma(1-\kappa) & g_5 \end{bmatrix}, |\mathbf{W}| = \begin{vmatrix} g_3 & 0 & 0 \\ -\sigma & g_4 & 0 \\ 0 & -\gamma(1-\kappa) & g_5 \end{vmatrix} = g_3 g_4 g_5$$

$$\therefore \quad \mathbf{W}^{-1} = \frac{1}{g_3 g_4 g_5} \begin{bmatrix} g_4 g_5 & 0 & 0 \\ \sigma g_5 & g_3 g_5 & 0 \\ \gamma(1-\kappa)\sigma & g_3\gamma(1-\kappa) & g_3 g_4 \end{bmatrix}$$

Now, the multiplication of the above values of F and W^{-1} gives

$$FW^{-1} = \begin{bmatrix} \frac{b\sigma}{N^0}\left(S^0 + (1-\varepsilon)V^0\right)\{g_5\omega_I + \gamma(1-\kappa)\omega_Q\} & \frac{bg_3}{N^0}\left(S^0 + (1-\varepsilon)V^0\right)\{g_5\omega_I + \gamma(1-\kappa)\omega_Q\} & g_3 g_4 \frac{b\omega_Q}{N^0}\left(S^0 + (1-\varepsilon)V^0\right) \\ 0 & 0 & 0 \\ 0 & 0 & 0 \end{bmatrix}$$

The average number of secondary infectious produced by a single infections in a susceptible population when vaccine intervention has been employed is referred to the effective reproduction number $R_0(v)$ [13]. Therefore, the spectral radius of the next generation matrix is $R_0(v)$ for the proposed model, and is given by

$$R_0(\nu) = \frac{b\sigma}{g_3 g_4 g_5 N^0}\left[S^0 + (1-\varepsilon)V^0\right]\{g_5\omega_I + \gamma(1-\omega_Q)\} \tag{12}$$

Putting the values of S^0 and V^0 in equation (12), we get

$$R_0(\nu) = \frac{b\sigma}{g_3 g_4 g_5 N^0}\left[\frac{(1-p)\Lambda}{g_1} + (1-\varepsilon)\frac{\Lambda\{pg_1 + (1-p)\nu\}}{g_1 g_2}\right]\{g_5\omega_I + \gamma(1-\omega_Q)\}$$

or

$$R_0(\nu) = \frac{b\sigma\mu G_1 \left[G_2 (1-\varepsilon) \{p g_1 + (1-p)\nu\}\right]}{(\mu+\nu) g_2 g_3 g_4 g_5} \tag{13}$$

where $G_1 = \{g_5\omega_I + \gamma(1-\omega_Q)\}$ and $G_2 = (1-p) g_2 = (1-p)\mu$.

3.5. Existence of Endemic Equilibrium (EE)

At the endemic equilibrium (EE), infection is always present in the system. Let $E^*(S^*, V^*, E^*, I^*, Q^*, R^*)$ be the endemic equilibrium point. Then, for EE, we have $\frac{dS}{dt} = 0$; $\frac{dV}{dt} = 0$; $\frac{dE}{dt} = 0$; $\frac{dI}{dt} = 0$; $\frac{dQ}{dt} = 0$, where $I^* \neq 0$.
For simplicity, we use $q = 1-p, 1-\epsilon = \epsilon_1, 1-\kappa = \kappa_1, d_1 = \beta + g_1, d_2 = (\beta_v + g_2)$.
Now, by $\left.\frac{dS}{dt}\right|_{E^*} = 0$, we have

$$S_* = \frac{(1-p)\Lambda + \eta R^*}{(\beta + g_1)} = \frac{q\Lambda + \eta R^*}{d_1} \tag{14}$$

By $\left.\frac{dV}{dt}\right|_{E^*} = 0$, we have

$$V^* = \frac{p\Lambda + \nu S^*}{(\beta_v + g_2)} = \frac{p\Lambda + \nu S^*}{d_2} \tag{15}$$

By $\left.\frac{dE}{dt}\right|_{E^*} = 0$, we have

$$E^* = \frac{\beta S^* + \beta_v V^*}{g_3} \tag{16}$$

By $\left.\frac{dI}{dt}\right|_{E^*} = 0$, we have

$$I^* = \frac{\sigma E^*}{g_4} \tag{17}$$

By $\left.\frac{dQ}{dt}\right|_{E^*} = 0$, we have

$$Q^* = \frac{(1-\kappa)\gamma}{g_5} I^* = \frac{\kappa_1\gamma}{g_5} I^* \tag{18}$$

By $\left.\frac{dR}{dt}\right|_{E^*} = 0$, we have

$$R^* = \frac{\gamma\kappa I^* + \tau Q^*}{g_6}$$

Substituting the value of Q^* from (18) in the above equation, we get

$$R^* = \left(\frac{\gamma\kappa g_5 + \gamma\kappa_1\tau}{g_5 g_6}\right) I^* \tag{19}$$

Again, substituting the value of R^* from (19) in (14) and (15), we respectively get

$$S^* = \frac{qg_5g_6\Lambda + \gamma\eta\left(\kappa g_5 + \kappa_1\tau\right) I^*}{d_1 g_5 g_6}$$

and

$$V^* = \frac{pd_1g_5g_6\Lambda + q\nu g_5g_6\Lambda + \gamma\nu\eta\left(\kappa g_5 + \kappa_1\tau\right) I^*}{d_1 d_2 g_5 g_6}$$

Now, substituting the values of S^* and V^* in (16), we get

$$E^* = \frac{\beta_v pd_1g_5g_6\Lambda + \left(\beta d_2 + \beta_v\nu\right)\left\{qg_5g_6\Lambda + \gamma\eta\left(\kappa g_5 + \kappa_1\tau\right) I^*\right\}}{d_1 d_2 g_3 g_5 g_6}$$

Again, substituting the value of E^* in equation (17), we get

$$I^* = \frac{\sigma}{g_4}\left[\frac{\beta_v pd_1g_5g_6\Lambda + \left(\beta d_2 + \beta_v\nu\right)\left\{qg_5g_6\Lambda + \gamma\eta\left(\kappa g_5 + \kappa_1\tau\right) I^*\right\}}{d_1 d_2 g_3 g_5 g_6}\right]$$

Hence, the EE is obtained as $E^*\left(S^*, V^*, E^*, I^*, Q^*, R^*\right)$, where

$$S^* = \frac{qg_5g_6\Lambda + \gamma\eta\left(\kappa g_5 + \kappa_1\tau\right) I^*}{\left(\beta + g_1\right) g_5 g_6},\ V^* = \frac{p\left(\beta + g_1\right) g_5g_6\Lambda + q\nu g_5g_6\Lambda + \gamma\nu\eta\left(\kappa g_5 + \kappa_1\tau\right) I^*}{\left(\beta + g_1\right)\left(\beta_v + g_2\right) g_5 g_6},$$

$$E^* = \frac{\beta_v p\left(\beta + g_1\right) g_5g_6\Lambda + \left(\beta\left(\beta_v + g_2\right) + \beta_v\nu\right)\left\{qg_5g_6\Lambda + \gamma\eta\left(\kappa g_5 + \kappa_1\tau\right) I^*\right\}}{\left(\beta + g_1\right)\left(\beta_v + g_2\right) g_3 g_5 g_6},$$

$$Q^* = \frac{\gamma\kappa_1}{g_5} I^* \text{ and } R^* = \left(\frac{\gamma\kappa g_5 + \gamma\kappa_1\tau}{g_5 g_6}\right) I^*$$

3.6. Stability Analysis of Disease-Free Equilibrium

Theorem 3. *The disease-free equilibrium point E_1 of the epidemic model* (1) *is locally asymptotically stable when $R_0 < 1$, otherwise unstable.*

Proof. For the disease free equilibrium, we take $\beta = b\left(\frac{\omega_I I^0 + \omega_Q Q^0}{N}\right) = 0$ and

$\beta_\nu = b(1-\varepsilon)\left(\frac{\omega_I I^0 + \omega_Q Q^0}{N}\right) = 0$. Therefore, the Jacobian matrix $J(E_1)$ at the DFE point E_1 is given by

$$J(E_1) = \begin{bmatrix} -g_1 & 0 & 0 & -\frac{b\omega_I S^0}{N^0} & -\frac{b\omega_Q S^0}{N^0} & \eta \\ \nu & -g_2 & 0 & -\frac{b(1-\varepsilon)\omega_I V^0}{N^0} & -\frac{b(1-\varepsilon)\omega_Q V^0}{N^0} & 0 \\ 0 & 0 & -g_3 & \frac{b\omega_I S^0}{N^0} + \frac{b(1-\varepsilon)\omega_I V^0}{N^0} & \frac{b\omega_Q S^0}{N^0} + \frac{b(1-\varepsilon)\omega_Q V^0}{N^0} & 0 \\ 0 & 0 & \sigma & -g_4 & 0 & 0 \\ 0 & 0 & 0 & \gamma(1-\kappa) & -g_5 & 0 \\ 0 & 0 & 0 & \gamma\kappa & \tau & -g_6 \end{bmatrix}$$

The characteristic equation $|J(E_1) - \lambda I| = 0$ of the system (1) gives us

$$\begin{vmatrix} -g_1-\lambda & 0 & 0 & -\frac{b\omega_I S^0}{N^0} & -\frac{b\omega_Q S^0}{N^0} & \eta \\ \nu & -g_2-\lambda & 0 & -\frac{b(1-\varepsilon)\omega_I V^0}{N^0} & -\frac{b(1-\varepsilon)\omega_Q V^0}{N^0} & 0 \\ 0 & 0 & -g_3-\lambda & \frac{b\omega_I S^0}{N^0} + \frac{b(1-\varepsilon)\omega_I V^0}{N^0} & \frac{b\omega_Q S^0}{N^0} + \frac{b(1-\varepsilon)\omega_Q V^0}{N^0} & 0 \\ 0 & 0 & \sigma & -g_4-\lambda & 0 & 0 \\ 0 & 0 & 0 & \gamma(1-\kappa) & -g_5-\lambda & 0 \\ 0 & 0 & 0 & \gamma\kappa & \tau & -g_6-\lambda \end{vmatrix} = 0$$

Substituting $A = \frac{b\omega_I S^0}{N^0} + \frac{b(1-\varepsilon)\omega_I V^0}{N^0}$ and $B = \frac{b\omega_Q S^0}{N^0} + \frac{b(1-\varepsilon)\omega_Q V^0}{N^0}$ and expanding the determinant along second, first and the fourth columns successively, we get three eigenvalues as : $\lambda_1 = -g_2, \lambda_2 = -g_1, \lambda_3 = -g_6$. The remaining eigenvalues are given by

$$-g_3g_4g_5 - (g_3g_4 + g_3g_5 + g_4g_5)\lambda - (g_3 + g_4 + g_5)\lambda^2 - \lambda^3 + \sigma\{g_5A + \lambda A + \gamma(1-\kappa)B\} = 0 \quad (20)$$

The last term of L.H.S. of equation (20) after simplification gives

$$\begin{aligned} \sigma\{g_5A + \lambda A + \gamma(1-\kappa)B\} &= \sigma\lambda A + \sigma[g_5A + \gamma(1-\kappa)B] \\ &= \sigma\lambda A + \frac{b\sigma\left[S^0 + (1-\varepsilon)V^0\right]\{g_5\omega_I + \gamma(1-\kappa)\omega_Q\}}{N^0 g_3g_4g_5} g_3g_4g_5 \\ &= \sigma\lambda A + R_0 g_3g_4g_5 \end{aligned}$$

Hence, the equation (20) reduces to the following form :
$\lambda^3 + (g_3 + g4 + g_5)\lambda^2 + (g_3g_4 + g_3g_5 + g_4g_5 - \sigma A)\lambda + g_3g_4g_5(1 - R_0) = 0$
which can also be written as follows:

$$\lambda^3 + a\lambda^2 + b\lambda + c = 0 \quad (21)$$

where $a = g_3 + g_4 + g_5 > 0,\ b = g_3g_4 + g_3g_5 + g_4g_5 - \sigma A > 0, \quad c = g_3g_4g_5(1 - R_0)$

Table 2: *Routh table* for the cubic equation (21) .

λ^3	1	b	0
λ^2	a	c	0
λ	$b-\frac{c}{a}$	0	0
1	c	0	0

Routh-Hurwitz criterion of order three [20, 24] implies that the three roots of (21) have negative real part if $a>0, b-\frac{c}{a}>0$ or $b>\frac{c}{a}, c>0$.

These criteria are satisfied only if $(1-R_0)>0$ i.e. $R_0<1$. Hence, all the roots of the characteristic equation of system (1) at the DFE point E_1 will have negative real parts if $R_0<1$.

Therefore, the DFE point is locally asymptotically stable when $R_0<1$, otherwise unstable.

3.7. Stability Analysis of Endemic Equilibrium

Theorem 4. *The endemic equilibrium point E^* of the epidemic model* (1) *is locally asymptotically stable if $R_0>1$ and inequalities* (20) *hold.*

Proof. The Jacobian matrix $J(E^*)$ at EE point E^* is given by

$$J(E^*) = \begin{bmatrix} -(\beta+g_1) & 0 & 0 & -\frac{b\omega_I S^*}{N} & -\frac{b\omega_Q S^*}{N} & \eta \\ \nu & -(\beta_v+g_2) & 0 & -\frac{b(1-\varepsilon)\omega_I V^*}{N} & -\frac{b(1-\varepsilon)\omega_Q V^*}{N} & 0 \\ \beta & \beta_v & -g_3 & \frac{b\omega_I S^*}{N}+\frac{b(1-\varepsilon)\omega_I V^*}{N} & \frac{b\omega_Q S^*}{N}+\frac{b(1-\varepsilon)\omega_Q V^*}{N} & 0 \\ 0 & 0 & \sigma & -g_4 & 0 & 0 \\ 0 & 0 & 0 & \gamma(1-\kappa) & -g_5 & 0 \\ 0 & 0 & 0 & \gamma\kappa & \tau & -g_6 \end{bmatrix}$$

$$= \begin{bmatrix} J_{11} & J_{12} & J_{13} & J_{14} & J_{15} & J_{16} \\ J_{21} & J_{22} & J_{23} & J_{24} & J_{25} & J_{26} \\ J_{31} & J_{32} & J_{33} & J_{34} & J_{35} & J_{36} \\ J_{41} & J_{42} & J_{43} & J_{44} & J_{45} & J_{46} \\ J_{51} & J_{52} & J_{53} & J_{54} & J_{55} & J_{56} \\ J_{61} & J_{62} & J_{63} & J_{64} & J_{65} & J_{66} \end{bmatrix}$$

Let us define $R_i=\sum_{j=1,j\neq i}^{6}|J_{ij}|, for \quad i=1,\ldots.6$. Then, we have

$$R_1 = \sum_{j=1,j\neq 1}^{6}|J_{ij}| = |J_{12}|+|J_{13}|+|J_{14}|+|J_{15}|+|J_{16}| = \frac{b\omega_I S^*}{N}+\frac{b\omega_Q S^*}{N}+\eta$$

$$R_2 = \sum_{j=1,j\neq 2}^{6}|J_{ij}| = |J_{21}|+|J_{23}|+|J_{24}|+|J_{25}|+|J_{26}| = \nu+\frac{b\varepsilon_1\omega_I V^*}{N}+\frac{b\varepsilon_1\omega_Q V^*}{N}$$

$$
\begin{aligned}
R_3 &= \sum_{j=1,j\neq 3}^{6} |J_{ij}| = |J_{31}| + |J_{32}| + |J_{34}| + |J_{35}| + |J_{36}| \\
&= \beta + \beta_v + \frac{b\omega_I S^*}{N} + \frac{b\varepsilon_1\omega_I V^*}{N} + \frac{b\omega_Q S^*}{N} + \frac{b\varepsilon_1\omega_Q V^*}{N} \\
R_4 &= \sum_{j=1,j\neq 4}^{6} |J_{ij}| = |J_{41}| + |J_{42}| + |J_{43}| + |J_{45}| + |J_{46}| = \sigma \\
R_5 &= \sum_{j=1,j\neq 5}^{6} |J_{ij}| = |J_{51}| + |J_{52}| + |J_{53}| + |J_{54}| + |J_{56}| = \gamma\kappa_1 \\
R_6 &= \sum_{j=1,j\neq 6}^{6} |J_{ij}| = |J_{61}| + |J_{62}| + |J_{63}| + |J_{64}| + |J_{65}| = \gamma\kappa + \tau
\end{aligned}
$$

Gershgorin stability theorem [4] states that the system will be stable if two conditions : $J_{ii} < 0$, and $R_i < |J_{ii}|$, for $i = 1, 2, \ldots 6$ are satisfied.

It can be observed that $J_{11} = -(\beta + g_1) < 0, J_{22} = -(\beta_\nu + g_2) < 0, J_{33} = -g_3 < 0, J_{44} = -g_4 < 0$, $J_{55} = -g_5 < 0, J_{66} = -g_6 < 0$.

Hence, the first condition of the Gershgorin stability theorem is satisfied.

Additionally, the following inequalities need to be hold in order for the second hypothesis of the Gershgorin stability theorem, $R_i < |J_{ii}|\,;\ i = 1, 2, \ldots 6$ to hold.

$$
\left.
\begin{aligned}
\frac{b\omega_I S^*}{N} + \frac{b\omega_Q S^*}{N} + \eta &< (\beta + g_1)\,, \\
\nu + \frac{b\varepsilon_1\omega_I V^*}{N} + \frac{b\varepsilon_1\omega_Q V^*}{N} &< (\beta_\nu + g_2) \\
\beta + \beta_v + \frac{b\omega_I S^*}{N} + \frac{b\varepsilon_1\omega_I V^*}{N} + \frac{b\omega_Q S^*}{N} + \frac{b\varepsilon_1\omega_Q V^*}{N} &< g_3 \\
\sigma &< g_4 \\
\gamma\kappa_1 &< g_5 \\
\gamma\kappa + \tau &< g_6
\end{aligned}
\right\} \qquad (22)
$$

Consequently,the endemic equilibrium point E^* of the epidemic model (1) is locally asymptotically stable when inequalities (22) holds.

4. Numerical Simulation, Results and Discussion

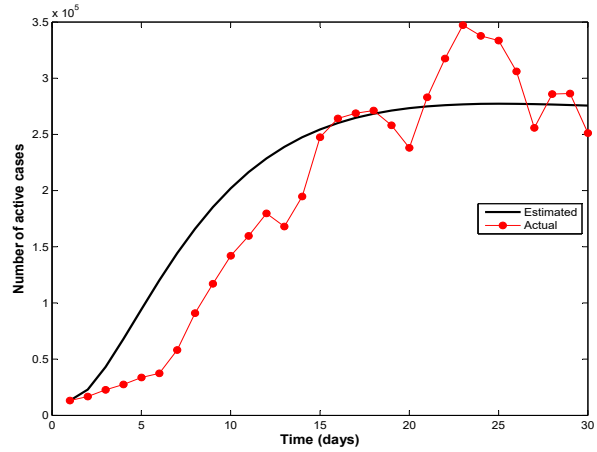

Figure 2: Model fitting with the active COVID-19 infective cases in India from December 30, 2021 to January 28, 2022.

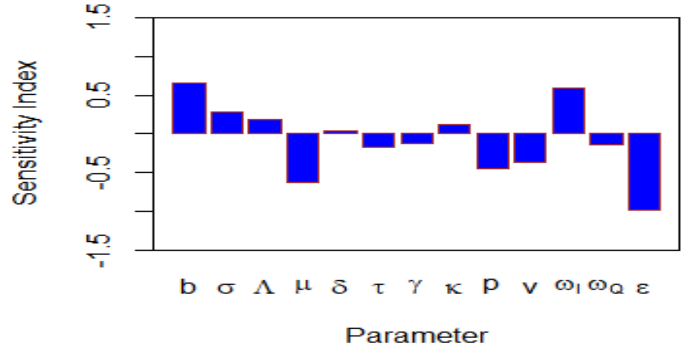

Figure 3: PRCCs showing the effect of varying the input parameters on $R_0\,(\nu)$.

The reported active infected cases and the vaccinated population in India are 6553 and 551,003,319 respectively by December 20, 2021 [31]. So, we set the initial population in the infected and vaccinated compartments for the simulation as $I(0) = 6563$ and $V(0) = 551,003,319$ respectively. The number of initial quarantined (hospitalized and home isolated) cases is considered as 20 % of the total

Table 3: Values of parameters used for the simulation of SVEIQR model

Parameter Value	**Source**
$\Lambda = 65937.74$	Estimated
$p = 0.4$	Assumed on the basis of WHO report
$\beta = 0.000432$	Estimated
$\mu = 0.0002$	[17]
$\delta = 0.00025$	[17]
$\sigma = 0.3$	[25]
$\nu = 0.3$	Assumed
$\eta = 0.011$	[23]
$\tau = 0.0701$	[11]
$\kappa = 0.05$	[8]
$b = 1.12$	[3]
$\gamma = 0.012$	[32]
$\varepsilon = 0.8$	Assumed
$\omega_I = 3.8$	Assumed
$\omega_Q = 1.3$	Assumed

active infected cases, and it is calculated as $Q(0) = 1313$. Since there is no information on the initial exposed population, which is believed to be twice as many as active infected cases, so we take E $(0) = 13126$. According to the record of Ministry of Statistics and Programme Implementation, the total population in India is 1,380,004,385 [18]. Hence, the initial population of the susceptible class is obtained as $S(0) = N - (V + E + Q + I + R) = 828,978,827$.

4.1. Model Fitting and Validation of Model

For model fitting and parameter estimation, we have worked with active COVID-19 cases data of India during the first stage of the third wave of COVID-19 and invented vaccination starting period (from December 20, 2021 to January 25, 2022). By the model fitting, we have estimated the values of parameters such as disease transmission rate, proportion of the recruitment individual who is vaccinated. The birth rate is (17.44/1000) per year for India and so it is reasonable to take the daily recruitment rate (Λ) as 65,937.74. Other parameter values are taken from the published literature. Using above initial conditions, available values of the parameters, we have fitted proposed model (1) and compared with the reported data of WHO daily dashboard of coronavirus (WHO, 2021) in Figure (2). We have estimated other key parameters including the effective reproduction number. Figure

(2) demonstrates the actual reported and the model estimated cases of confirmed COVID-19 cases. The graph confirms that the model is valid.

4.2. Sensitivity Analysis for R_0

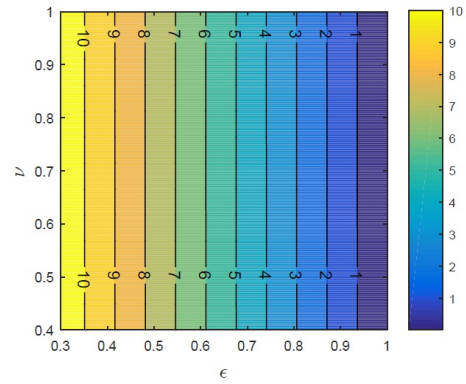

Figure 4: Contour plot of $R_0(\nu)$ with vaccine coverage (ν) and efficacy (ϵ).

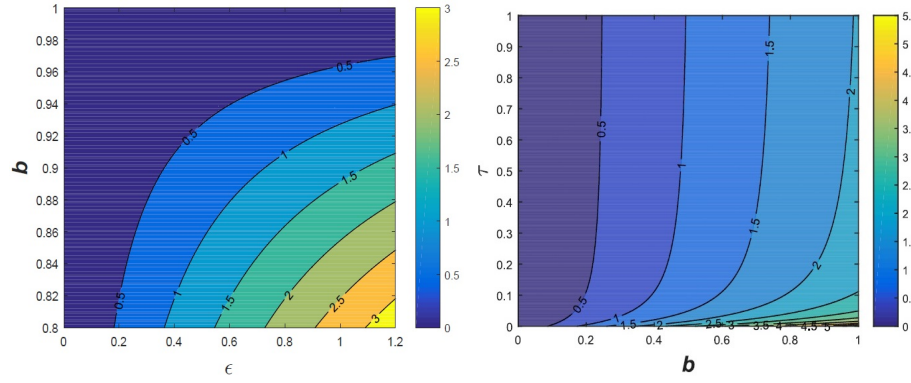

Figure 5: Contour plot of $R_0(\nu)$ with (i) effective contact rate (b) and efficacy (ϵ) (left panel) ; (ii) effective contact rate (b) and treatment rate (τ) (right panel).

We calculate sensitivity indices with regard to the corresponding parameters as the initial disease transmission is exclusively related to $R_0(\nu)$. Using the Latin hypercube scheme and Partial rank correlation coefficients (PRCCs), we undertake sensitivity analysis [22]. The Figure (3) depicts PRCCs that demonstrate how altering the input parameters affect $R_0(\nu)$. Hence, the effective reproduction number $R_0(\nu)$ is seen to increase for all parameters with positive PRCCs and decline for all parameters with negative PRCCs as their values are increased. The model's

most influential parameters are those with big PRCC values (> 0.5 or < -0.5) and correspondingly low p-values (< 0.05). The most important parameters can be found by examining Figure (3). Model parameters that should be aimed to stop the spread of the disease are effective contact rate (b), the infection reduction (vaccine efficacy) of vaccinated individuals (ε), the exist rates from the exposed and infected classes σ and γ. Additionally, b is discovered to be the parameter with the highest positive sensitivity. As their absolute values of PRCCs are higher than equivalent values of other parameters, parameters b, ω_I and ε have a strong correlation with $R_0(\nu)$. Moreover, p, μ and ν are the other sensitive parameters that negatively affect $R_0(\nu)$. The contour plots (4) and (5) provide the clearest representation of the patterns of the change in the value of $R_0(\nu)$. So, it follows that strengthening the relevance of isolation and vaccination quickly is the best course of action for disease control.

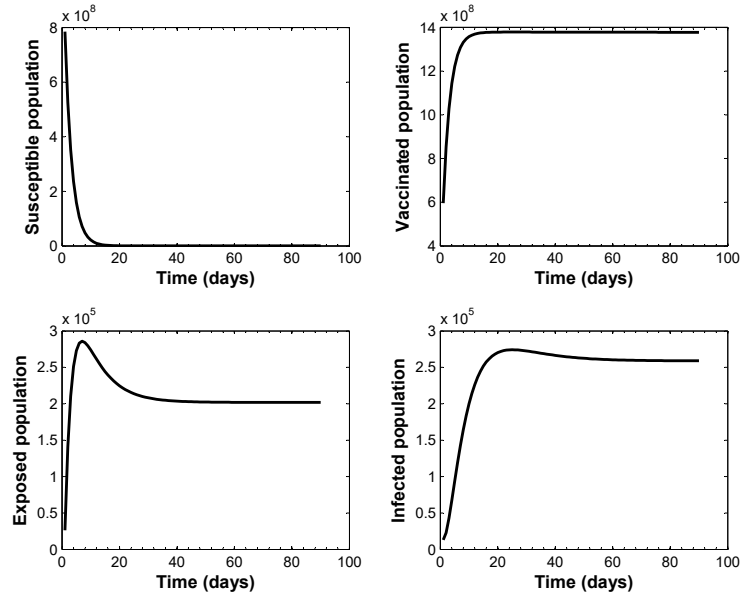

Figure 6: Dynamical behavior of the disease taking parameter values in Table 1 for $R_0(\nu) > 1$.

4.3. Disease Dynamics

Using model parameter values in Table 3, we get $R_0(\nu) = 1.4280 > 1$. In order to study the disease dynamics and validation of proposed model (1), we simulate the daily coronavirus infective, susceptible, exposed and vaccinated cases for the period of 90 days (three month) starting from the initial date of our study

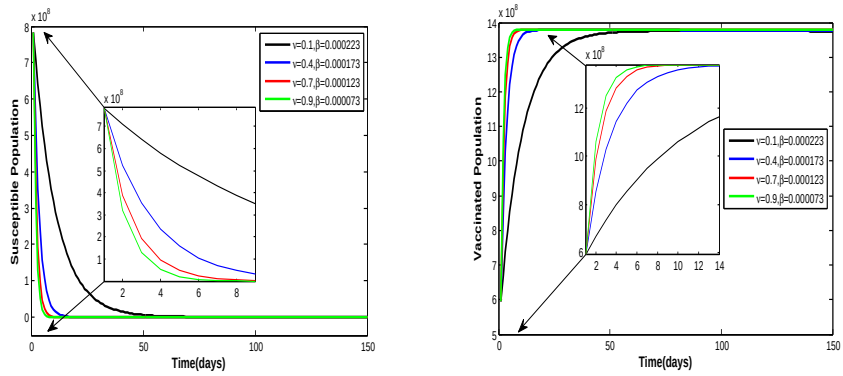

Figure 7: Dynamical behavior of the susceptible and vaccinated population with different levels of control strategies.

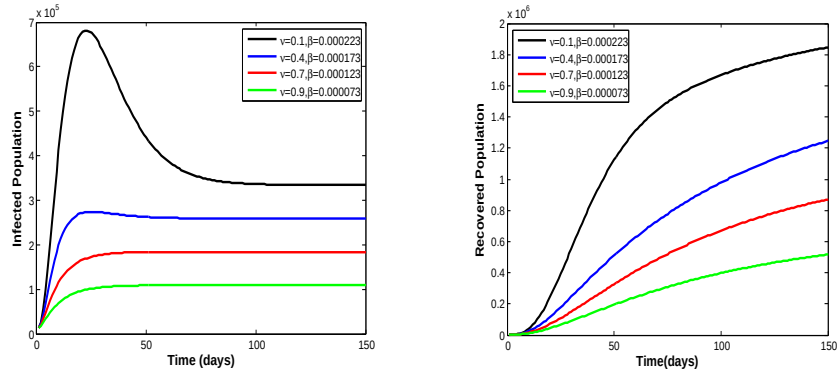

Figure 8: Dynamical behavior of the infected and recovered population with different levels of control strategies.

period December 20, 2021 using the parameter values in the Table 3. Clearly, the estimated cumulative coronavirus cases by the model remains increasing in the next 90 days unless other extra intervention measures are induced in the society. This represents the dynamics of the disease in present scenario.

To study the nature of dynamics of coronavirus diseases, we simulate our model (1) for a long-term (180 days) for different values of the parameters ν and β with remaining parameters listed in the Table 3. Here, ν and β represent the various level (degree) of interventation measures of control parameters.

Figures (7) and (8) depict the graphical representation of the simulation of the COVID-19 model (1) as a function of time with and without further control strategies. The long-term impact of the interventions with expected values of

the parameters seems to be successful to mitigate the spread of the disease in the total number of individuals in the disease-infected classes and the vaccinated compartment.

5. Conclusion

Our model simulations suggest that the novel coronavirus disease has potential to exhibit increase exponentially with high rate in the initial stage and remains as endemic disease for a long period in the society with existing level of implementation of non-pharmaceutical and medical intervention. But the situation can be controlled by the implementation two control measures; first maintaining the effectiveness of isolation or quarantined and social distances that decreases the transmission rate; second increasing the rate of full dose (booster dose) of the vaccine. Long-term model simulation with the control measure illustrates the sufficient optimum rate of control measures able to effective control in a community and may eliminate the coronavirus transmission in the long-term.

Future studies of the research can include some more compartments such as dead class, immigrated population class to make the broad model. Instead of taking the whole of India as the study population, each state of India may be considered separately for better policies of controlling the spread of the COVID-19.

References

[1] Anirudh A., Mathematical modeling and the transmission dynamics in predicting the COVID-19—what next in combating the pandemic, Infect Dis Model, 5 (2020), 366–374.

[2] Annas S., Pratama MI, Rifandi M., Sanusi W., Side S., Stability analysis and numerical simulation of SEIR model for pandemic covid-19 spread in Indonesia, Chaos, Solitons & Fractals, (2020), 110072.

[3] Babaei A., Jafari H., Banihashemi S., and Ahmadi M., Mathematical analysis of a stochastic model for the spread of Coronavirus, Chaos, Solitons & Fractals, 145 (2021), article 110788.

[4] Bejarano, D., Ibarguen-Mondragon, E. and Gomez-Hernandez, E. A., A stability test for non linear systems of ordinary differential equations based on the gershgorin circles, Contemporary Engineering Sciences, 11 (91) (2018), 4541-4848.

[5] Bhadauria, A. S., Verma, V. S., Verma, V. and Rana, V., An SIQV mathematical model on COVID-19 with virus population in the environment, Mathematics in Engineering, Sciences & Aerospace (MESA), 13 (1), (2022).

[6] Birkhoff, G. and Rota, G. C., Ordinary Differential Equations, Wiley, Hoboken, 1989.

[7] Chen S., Prettner K., Kuhn M., Geldsetzer P., Wang C., Bärnighausen T., et al., Climate and the spread of COVID-19, Sci Rep, 11 (2021), 9042.

[8] Deressa C. T., Mussa Y. O., and Duressa G. F., Optimal control and sensitivity analysis for transmission dynamics of coronavirus, Results in Physics, 19 (2020), article 103642.

[9] Diekmann O., Heesterbeek J. A., and J. A. Metz, On the definition and the computation of the basic reproduction ratio R_0 in models for infectious diseases in heterogeneous populations, Journal of Mathematical Biology, 28 (4) (1990), 365–382.

[10] Dorigatti I., Cauchemez S., Ferguson NM., Increased transmissibility explains the third wave of infection by the 2009 H1N1 pandemic virus in England, Proc Natl Acad SciU S A, 110 (2013), 13422-7.

[11] Garba S. M., Lubuma J. M., and Tsanou B., Modeling the transmission dynamics of the COVID-19 pandemic in South Africa, Mathematical Biosciences, 328 (2020), article 108441.

[12] Han E., Tan MM., Turk E., Sridhar D., Leung GM., Shibuya K., et al., Lessons learned from easing COVID-19 restrictions: An analysis of countries and regions in the Asia Pacific and Europe, Lancet, 396 (2020), 1525-1534.

[13] Hethcote, H. W., The Mathematics of Infectious Diseases, SIAM Review, 42 (2000), 599-653.

[14] Huang C., Wang Y., Li X., Ren L., Zhao J., Hu Y., Zhang L., Fan G., Xu J., Gu X., et al., Clinical features of patients infected with 2019 novel coronavirus in Wuhan, China, The lancet, 395 (10223) (2020), 497–506.

[15] Kermack W. O., McKendrick A. G., A contribution to the mathematical theory of epidemics, Proc R Soc Lond, 115 (772) (1927), 700–721.

[16] Kunwar L. B. and Verma V. S., Mathematical modelling of COVID-19 pandemic in Nepal using logistic growth model, International Journal of Graduate Research and Review, 7 (1) (2021), 17-24.

[17] Mandal, M., Jana, S., Nandi, S. K., Khatua, A., Adak, S. and Kar, T. K., A Model Based Study on the Dynamics of COVID-19: Prediction and Control, Chaos, Solitons and Fractals, 136 (2020), Article ID: 109889.

[18] Ministry of Health and Family Welfare Press release 16 Jan 2021. Available from: https://pib.gov.in/PressReleasePage. asp?PRID=1689018 accessed on May 30, 2021.

[19] Ministry of Statistics and Programme implementation, UN(World Population Prospects 2019), 09 Dec 2021, https://statisticstimes.com/demographics/country/india-population.php.

[20] Routh E. J., A treatise on the stability of a given state of motion, particularly 2 steady motion, Macmillan & Co., London, 1877.

[21] Saeed H., Osama H., Madney Y. M., Harb H. S., Abdelrahman M. A., Ehrhardt C., Abdelrahim M. A. Ehrhardt C., COVID-19; current situation and recommended interventions, Int J Clin Pract, (2021). https:// doi. org/ 10. 1111/ ijcp. 13886

[22] Sanchez M. A., and Blower S. M., Uncertainty and sensitivity analysis of the basic reproductive rate: tuberculosis as example, American journal of epidemiology, 145 (12) (1997), 1127-1137.

[23] Shakhany M. Q. and Salimifard K., Predicting the dynamical behaviour of COVID-19 epidemic and the effect of control strategies, Chaos, Solitons & Fractals, 146 (2021), article 110823.

[24] Sigal R., Algorithms for the Routh-Hurwitz stability test, Mathematical and Computer Modelling, 13 (8) (1990), 69-77.

[25] Tang B., Wang X., Li Q. et al., Estimation of the transmission risk of the 2019-nCoV and its implication for public health interventions, Journal of Clinical Medicine, 9 (2), (2020), 462.

[26] Taubenberger J. K., Morens D. M., Influenza: The mother of all pandemics, Emerg Infect Dis, 12 (2006), 15-22.

[27] The Times of India, 20 cases of new Delta-plus variant in India, 8 in Maharashtra., Available from: https://timesofindia.indiatimes.com/city/mumbai/20-cases-of-new- delta-

plusvariant-in-India -8-in-Maharashtra/articles how/83700399.cms, accessed on May 20, 2021.

[28] Vaidyanathan G., Coronavirus variants are spreading in India - what scientists know so far, Nature, 593 (2021), 321-332.

[29] Van den Driessche, P., Watmough, J., Reproduction Numbers and Sub-Threshold Endemic Equilibria for Compartmental Models of Disease Transmission, Math Biosci, 180 (2002), 29-48.

[30] Verma V. S., Kunwar L.B., Bhadauria, A. S. and Rana V., An SVIQR epidemic model for COVID-19, South East Asian Journal of Mathematics and Mathematical Sciences, 18 (3) (2022), 101-122.

[31] World Health Organization,WHO Coronavirus (COVID-19) Dashboard, Available from:
https://covid19.who.int/region/searo/country/in, accessed on May 31, 2021.

[32] Yavuz M., Cosar F. O., Gunay F. and Ozdemir F. N. A., A new mathematical modeling of the COVID-19 pandemic including the vaccination campaign, Open Journal of Modelling and Simulation, 9 (3) (2021), 299-321.

[33] Zeb A., Alzahrani E., Erturk V.S., Zaman G., Mathematical model for coronavirus disease 2019 (covid-19) containing isolation class, Biomed Res Int, 2020.